Nonlinear envelope equation for broadband optical pulses in quadratic media

Matteo Conforti, Fabio Baronio, and Costantino De Angelis
CNISM and Dipartimento di Ingegneria dell'Informazione, Università di Brescia, Via Branze 38, I-25123 Brescia, Italy
(Received 7 January 2010; published 21 May 2010)

We derive a nonlinear envelope equation to describe the propagation of broadband optical pulses in second-order nonlinear materials. The equation is first order in the propagation coordinate and is valid for arbitrarily wide pulse bandwidth. Our approach goes beyond the usual coupled wave description of $\chi^{(2)}$ phenomena and provides an accurate modeling of the evolution of ultra-broadband pulses also when the separation into different coupled frequency components is not possible or not profitable.

DOI: 10.1103/PhysRevA.81.053841 PACS number(s): 42.65.Ky, 42.25.Bs, 42.65.Re

I. INTRODUCTION

The analysis of optical pulse propagation typically involves the definition of a complex envelope whose variation is supposed to be "slow" with respect to the oscillation of a carrier frequency ("slowly varying envelope approximation," SVEA [1]). In the frequency domain this assumption is equivalent to requiring that the bandwidth of the envelope is narrow with respect to the carrier frequency. Different works showed that it is possible to extend the validity of a proper generalization of the envelope equation [for example, the "nonlinear envelope equation" (NEE) of Brabec and Krausz] to pulse duration down to the single optical oscillation cycle [2–6] and to the generation of high-order harmonics [7]. When second-order nonlinearities are considered, the usual approach is to write coupled equations for the separated frequency bands relevant for the process [8–10]. However, when ultra-broadband $\chi^{(2)}$ phenomena take place, the different frequency bands might merge, generating a single broad spectrum, as observed in recent experiments [11]. Obviously in these cases the coupled NEE description of the propagation fails due to the overlapping between different frequency bands.

In this article, thanks to a proper definition of the envelope and of the nonlinear polarization, we provide a single wave envelope equation to describe ultra-broadband $\chi^{(2)}$ interactions. To date such a model is not available and the only way to numerically describe phenomena as those reported in Ref. [11] is to solve directly Maxwell equations in the time domain, with an immense computational burden. Our equation, besides providing a simple and powerful tool for analytical treatment due to its simplicity, can be easily solved with a modest computational effort and can be easily generalized to include other kinds of nonlinearities such as Kerr or Raman.

II. BROADBAND $\chi^{(2)}$ ENVELOPE EQUATION

As far as the linear dispersive terms are concerned, our derivation of the envelope equation builds upon the work of Brabec and Krausz [2], which carries to a simple model that was shown (theoretically and experimentally) to be accurate in most situations. Starting from Maxwell's equations (written in MKS units) and neglecting transverse dimensions (i.e., considering the propagation of plane waves), we can obtain the $1+1$D wave equation for the electric field $E(z,t)$:

$$\frac{\partial^2 E(z,t)}{\partial z^2} - \frac{1}{c^2}\frac{\partial^2}{\partial t^2}\int_{-\infty}^{+\infty} E(z,t')\varepsilon(t-t')dt' = \frac{1}{\varepsilon_0 c^2}\frac{\partial^2}{\partial t^2}P_{\mathrm{NL}}(z,t), \tag{1}$$

which can be written in the frequency domain by defining the Fourier transform $\mathcal{F}[E](\omega) = \hat{E}(\omega) = \int_{-\infty}^{+\infty} E(t)e^{-i\omega t}dt$:

$$\frac{\partial^2 \hat{E}(z,\omega)}{\partial z^2} + \frac{\omega^2}{c^2}\hat{\varepsilon}(\omega)\hat{E}(z,\omega) = -\frac{\omega^2}{\varepsilon_0 c^2}\hat{P}_{\mathrm{NL}}(z,\omega), \tag{2}$$

where c is the vacuum velocity of light, ε_0 is the vacuum dielectric permittivity, $\hat{\varepsilon}(\omega) = 1 + \hat{\chi}(\omega)$, and $\hat{\chi}(\omega)$ is the linear electric susceptibility.

We consider now the electric field E and the nonlinear polarization P_{NL} as the product of a complex envelope and a carrier wave $E(z,t) = A(z,t)/2e^{i\omega_0 t - i\beta_0 z} + \mathrm{c.c.}$, $P_{\mathrm{NL}}(z,t) = A_p(z,t)/2e^{i\omega_0 t - i\beta_0 z} + \mathrm{c.c.}$ [which in frequency domain reads $\hat{E}(z,\omega) = \hat{A}(z,\omega-\omega_0)/2e^{-i\beta_0 z} + \hat{A}^*(z,-\omega-\omega_0)/2e^{i\beta_0 z}$], where ω_0 is a reference frequency, $\beta_0 = \mathrm{Re}[k(\omega_0)]$, and $k(\omega) = (\omega/c)\sqrt{\hat{\varepsilon}(\omega)}$ is the propagation constant.

We devote particular care to the definition of the complex envelope, in order to avoid any assumption on the frequency extent of the signals. Previously it was taken for granted that the band of the envelope is "narrow" in some sense. In the following we shall see that, for quadratically nonlinear media, a proper definition of the envelope is critical. As usual in the theory of modulation [12], we define the analytic representation of the electric field as

$$\tilde{E}(z,t) = E(z,t) + i\mathcal{H}[E](z,t), \tag{3}$$

where

$$\mathcal{H}[E](z,t) = \frac{1}{\pi}\mathrm{P}\int_{-\infty}^{+\infty}\frac{E(z,t')}{t-t'}dt' \tag{4}$$

is the Hilbert transform of the electric field (where P indicates the Cauchy principal value of the integral). The Fourier transform of the analytic signal reads

$$\hat{\tilde{E}}(z,\omega) = \begin{cases} 2\hat{E}(z,\omega) & \text{if } \omega > 0, \\ \hat{E}(z,0) & \text{if } \omega = 0, \\ 0 & \text{if } \omega < 0, \end{cases} \tag{5}$$

that is, a signal that contains only the positive frequency content of the electric field. Because $E(z,t)$ is real, its Fourier transform has Hermitian symmetry, so that only the positive (or the negative) frequencies carry information, and we can write

$$\hat{E}(z,\omega) = \tfrac{1}{2}\hat{\tilde{E}}(z,\omega) + \tfrac{1}{2}\hat{\tilde{E}}^*(z,-\omega), \tag{6}$$

and eventually we can define the complex electric field envelope as

$$A(z,t) = \tilde{E}(z,t)e^{-i\omega_0 t + i\beta_0 z}, \tag{7}$$

that is, the inverse Fourier transform of the positive frequency content of E shifted toward the low-frequency part of the spectrum by an amount ω_0. *It is worth noting that no approximations on the frequency extent of the envelope has been done*, and so $\mathrm{supp}\{\hat{A}(z,\omega)\} = (-\omega_0,+\infty)$.

Substitution of expressions of $\hat{E}(z,\omega)$ and $\hat{P}_{\mathrm{NL}}(z,\omega)$ in Eq. (2), Taylor-expansion of $k(\omega)$ about ω_0, application of the slowly evolving wave approximation (SEWA, that is, the neglect of the second spatial derivative in the coordinate system moving at the group velocity at the reference frequency), followed by an inverse Fourier transform yields [1–3]

$$\frac{\partial A(z',\tau)}{\partial z'} + iDA(z',\tau) = -i\frac{\omega_0^2}{2\beta_0 c^2 \varepsilon_0}\left(1 - \frac{i}{\omega_0}\frac{\partial}{\partial \tau}\right)A_p(z',\tau), \tag{8}$$

where $D = \sum_{m=2}^{\infty} \frac{1}{m!}k_m(-i\frac{\partial}{\partial t})^m$, $k_m = \frac{\partial^m k}{\partial \omega^m}(\omega_0)$, $z' = z$, and $\tau = t - k_1 z$ is the coordinate system moving at the reference group velocity.

The key assumptions exploited are $|\frac{\partial A}{\partial z'}| \ll \beta_0|A|$ and $|\frac{\beta_0 - \omega_0 k_1}{\beta_0}| \ll 1$. It is worth noting that when the latter requirement is accomplished, SEWA does not explicitly impose a limitation on pulse duration and bandwidth. Far from resonances, this requirement is fulfilled in the majority of parametric processes in which all waves propagate in the same direction.

We now consider an instantaneous second-order $\chi^{(2)}$ nonlinearity, giving rise to the following nonlinear polarization:

$$\begin{aligned} P_{\mathrm{NL}}(z,t) &= \varepsilon_0 \chi^{(2)} E(z,t)^2 \\ &= \varepsilon_0 \chi^{(2)} \mathrm{Re}[A(z,t)e^{i\omega_0 t - i\beta_0 z}]^2 \\ &= \frac{\varepsilon_0 \chi^{(2)}}{4}[A^2 e^{2i\omega_0 t - 2i\beta_0 z} + A^{*2} e^{-2i\omega_0 t + 2i\beta_0 z} + 2|A|^2]. \end{aligned} \tag{9}$$

We assumed an instantaneous (frequency-independent) nonlinearity since the dispersion of the second-order nonlinear coefficient is very weak. However, the frequency dependence of $\chi^{(2)}$ can be easily inserted in our model, as done previously for cubic nonlinearities [1]. It is worth noting that, due to the definition of A, the first (second) term in the square brackets contains only positive (negative) frequencies, whereas the third has both. It is now apparent that it is impossible to separate the nonlinear polarization in two distinct and "narrow" bands for the positive and negative frequencies, as common in cubic media. Moreover, the neglect of the third term leads to totally wrong results. (This term is responsible for difference frequency generation.)

By going through the steps (3)–(7) we can instead correctly define the nonlinear polarization envelope:

$$\begin{aligned} A_p(z,t) &= \tilde{P}_{\mathrm{NL}}(z,t)e^{-i\omega_0 t + i\beta_0 z} \\ &= \frac{\varepsilon_0 \chi^{(2)}}{2}[A^2 e^{i\omega_0 t - i\beta_0 z} \\ &\quad + (|A|^2 + i\mathcal{H}[|A|^2])e^{-i\omega_0 t + i\beta_0 z}]. \end{aligned} \tag{10}$$

Before inserting Eq. (10) into Eq. (8), the term $|A|^2$ in Eqs. (9) and (10) deserves further comment, since it is centered around zero in the frequency domain. In particular to obtain the nonlinear polarization envelope in Eq. (10) we had to filter out the negative frequency components of $\hat{P}_{\mathrm{NL}}(\omega)$, as done for $\hat{E}(\omega)$. We note however that (i) $\hat{A}(z,\omega-\omega_0)$ does not contain any negative frequencies by definition, (ii) P_{NL} is a small perturbation to linear polarization, and (iii) negative frequencies cannot be phase-matched. It follows that the task of filtering the negative frequency components of $|A|^2$ can be left to the propagation equation instead of having it explicitly in the definition of $A_p(z,t)$. In other words, when inserting Eq. (10) into Eq. (8), we can write $|A|^2 + i\mathcal{H}[|A|^2] \approx 2|A|^2$. We have checked numerically the good accuracy of this approximation. Even if this approximation is not necessary in the numerical solution (for it is straightforward to calculate the exact nonlinear polarization envelope in the frequency domain), it is suitable to obtain a simple and manageable model for further analytical investigations.

The NEE for $A = A(z',\tau)$ becomes

$$\begin{aligned} \frac{\partial A}{\partial z'} + iDA = -i\frac{\chi^{(2)}\omega_0^2}{4\beta_0 c^2}\left(1 - \frac{i}{\omega_0}\frac{\partial}{\partial \tau}\right)[A^2 e^{i\omega_0\tau - i(\beta_0 - k_1\omega_0)z'} \\ + 2|A|^2 e^{-i\omega_0\tau + i(\beta_0 - k_1\omega_0)z'}], \end{aligned} \tag{11}$$

or, performing derivatives, we have

$$\begin{aligned} \frac{\partial A}{\partial z'} + iDA = -i\frac{\chi^{(2)}\omega_0^2}{4\beta_0 c^2}\left[\left(2A^2 - \frac{2i}{\omega_0}A\frac{\partial A}{\partial \tau}\right)e^{i\omega_0\tau - i(\beta_0 - k_1\omega_0)z'}\right. \\ \left. - \frac{4i}{\omega_0}\mathrm{Re}\left(A^*\frac{\partial A}{\partial \tau}\right)e^{-i\omega_0\tau + i(\beta_0 - k_1\omega_0)z'}\right]. \end{aligned} \tag{12}$$

Equation (11) or (12) constitutes the main result of this article. This nonlinear envelope equation, which is first order in the propagation coordinate, provides a powerful means of describing light pulse propagation in dispersive quadratically nonlinear media.

Starting from Eq. (11) it is straightforward to show that our equation conserves the total energy of the field [i.e., $\frac{d}{dz'}\int_{-\infty}^{+\infty}|A(z',\tau)|^2 d\tau = 0$]. It can also be shown that the total energy is conserved even if the nonapproximated nonlinear polarization envelope A_p [Eq. (10)] is used.

III. NUMERICAL RESULTS

We solved Eq. (11) by a split-step Fourier method exploiting the fourth-order Runge-Kutta scheme for the nonlinear step.

In order to show the validity of our equation, we simulated the propagation of a femtosecond pulse in a $L = 5$ mm long periodically poled lithium tantalate sample (PPLT). To model the refractive index dispersion we employed a Sellmeier model fitted from experimental data [13] and a nonlinear coefficient of $d_{33} = \chi^{(2)}_{\mathrm{LT}}/2 = 10.6$ pm/V. In the numerical code we

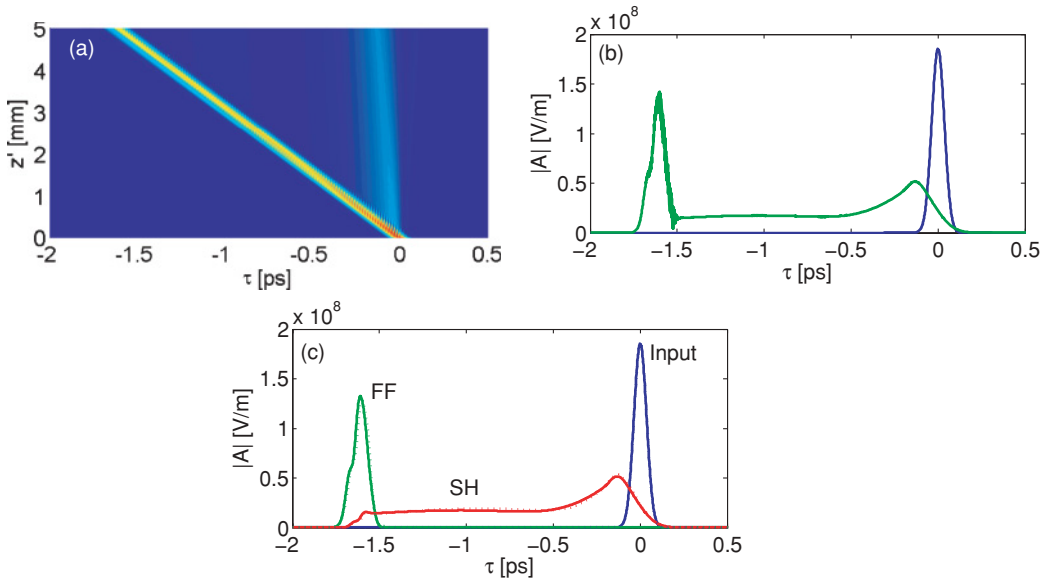

FIG. 1. (Color online) Propagation of a femtosecond pulse in a PPLT crystal. (a) Evolution of the field amplitude $|A|$ from numerical solution of Eq. (11). (b) Electric field amplitude at the crystal output. (c) Comparison between coupled wave solution (dotted curves) and $|A|$ filtered around fundamental and second harmonic (solid curves). The initial pulse has Gaussian shape and the parameters are $T = 60$ fs, $I = 10$ GW/cm^2, $\lambda_{\text{in}} = 1400$ nm, $\lambda_0 = 2\pi c/\omega_0 = 700$ nm, and $d_{33} = \chi^{(2)}_{\text{LT}}/2 = 10.6$ pm/V.

inserted the exact dispersion relation $k(\omega)$. We assumed a first-order quasi-phase-matching (QPM) grating, with a period $\Lambda = 17.4$ μm. We thus allowed a periodic variation of the nonlinear coefficient $\chi^{(2)} = \chi^{(2)}(z) = 2/\pi\, \chi^{(2)}_{\text{LT}} e^{i2\pi/\Lambda z} + \text{c.c.}$ We injected a $T = 60$ fs FWHM long Gaussian pulse, centered around 1400 nm, with $I = 10$ GW/cm^2 peak intensity. The corresponding residual phase mismatch is $\Delta k = 2k(\omega_{\text{in}}) - k(2\omega_{\text{in}}) = 10\,000$ m^{-1}, where ω_{in} is the carrier frequency of the input pulse. In the simulation we set the reference frequency ω_0 to be equal to the second harmonic of the input pulse: in this way the second harmonic is stationary in the reference frame (z', τ).

Figure 1(a) shows the evolution of the electric field envelope amplitude $|A|$ from the numerical solution of Eq. (11). We can see the typical scenario of the propagation of femtosecond pulses in a highly group velocity mismatched (GVM) process: The fundamental frequency (FF) pulse generates its second harmonic (SH) during propagation, and the generated SH pulse has the typical shape of an initial peak followed by a long tail, whose duration is fixed by the product between group velocity mismatch and crystal length. Figure 1(b) shows the electric field envelope amplitude at the end of the crystal. One sees a peak that corresponds to the faster frequency components located around the FF, followed by a long tail that ends with a second lower peak. This long pulse corresponds to the generated SH components. The SH pulse is smooth, indicating that no beating with eventual FF components is present, whereas in the residual FF pulses centered around $\tau \approx -1.6$ ps, there is a clear fast oscillation, indicating that FF and SH components are superimposed.

To test the results, we simulated the same setup with a standard coupled wave model [14], by inserting the values of first- and second-order dispersion evaluated at the FF and the SH. To compare the results we filtered A around the FF and the SH. Figure 1(c) shows the electric field amplitudes at the end of the crystal. The results of the two models are practically indistinguishable. It is worth noting that this simulation shows the validity of Eq. (11) over a bandwidth of ω_0.

As a second example we consider the propagation of a femtosecond pulse into a highly mismatched periodically poled lithium niobate (PPLN) sample, which was demonstrated experimentally to generate an octave-spanning supercontinuum spectral broadening [11]. To model the refractive index dispersion we employed a Sellmeier model fitted from experimental data [15] and a nonlinear coefficient of $d_{33} = \chi^{(2)}_{\text{LN}}/2 = 27$ pm/V. In the numerical code we inserted the exact dispersion relation $k(\omega)$. We dropped the imaginary part of $k(\omega)$ since linear absorption is negligible in the band of interest. We assumed a QPM grating with a period $\Lambda = 30$ μm (phase matched for second harmonic generation at around 2 μm fundamental wavelength). We included higher order QPM terms, since the huge bandwidth can phase-match different spatial harmonics. We injected a $T = 50$ fs FWHM long Gaussian pulse, centered around 1580 nm, with $I = 15$ GW/cm^2 peak intensity. In the simulation we set the reference wavelength to $\lambda_0 = 700$ nm. Figure 2(a) shows the evolution of the spectrum during the propagation into a $L = 7$ mm crystal. We can see a consistent broadening and redshift of the FF part of the spectrum that, at the end of the crystal, reaches an octave-spanning bandwidth from 1200 to 3000 nm. We can also see the generation of spectral components at the second and third harmonics. At the second harmonic the spectrum initially broadens and has an evolution ruled by highly mismatched second harmonic generation (SHG). When the FF broadening reaches the first-order quasi-phase-matching wavelength at around 2 μm, the more efficient conversion process generates a spike at around 1 μm. Figure 2(b) shows the visible and the near-infrared (NIR) part of the spectrum at

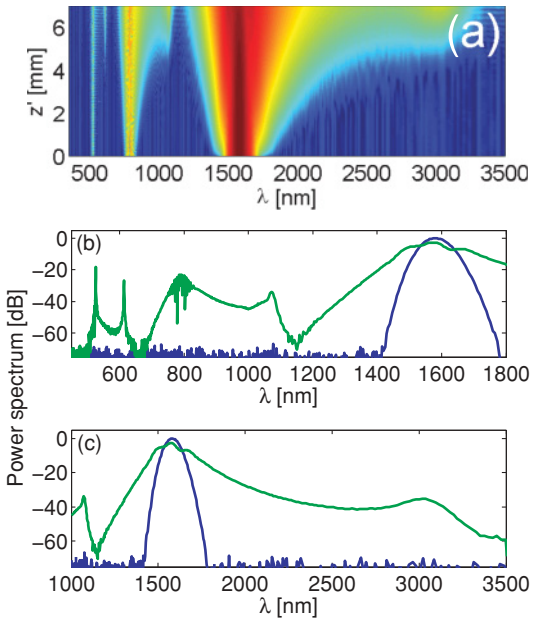

FIG. 2. (Color online) Propagation of a femtosecond pulse into a PPLN sample. (a) Evolution of the power spectrum (in dB) from numerical solution of Eq. (11). (b) Power spectrum at the crystal output in the visible and NIR range. (c) Power spectrum at the crystal output in the infrared range. The division into separate spectral regions is made to facilitate the comparison with experimental data [11]. The initial pulse has Gaussian shape and the parameters are $T = 50$ fs, $I = 15$ GW/cm^2, $\lambda_{in} = 1580$ nm, $\lambda_0 = 2\pi c/\omega_0 = 700$ nm, and $d_{33} = \chi^{(2)}_{\mathrm{LN}}/2 = 27$ pm/V.

the crystal output. We can see a broadband second and third harmonic of the broadened laser spectrum and the presence of some spikes given by the quasi-phase-matching of high-order spatial harmonics of the grating. We verified that the two spikes at the third harmonic correspond to the third-order QPM SHG (614 nm) and to the direct third harmonic generation (526 nm). We can also see a spectral overlap between the harmonics of the broadened laser spectrum that can be exploited to achieve carrier-envelope-offset phase slip stabilization [11], which is of paramount importance for frequency metrology applications.

Figure 2(c) shows the infrared spectrum at the output. This spectrum exhibits more than an octave spanning between 1300 and 3000 nm at the −40 dB spectral power level with respect to the peak power level. The spectral components near the zero GVM wavelength around 3000 nm are generated more efficiently due to phase-matched parametric generation.

All the features described here compare surprisingly well with the experimental results of Langrock *et al.* [11], even if we simulate a slightly different environment. In fact we use a bulk PPLN sample and not a reverse proton exchange (RPE) PPLN waveguide. The effect of the waveguide is to slightly modify the power levels and the crystal dispersion; a detailed simulation of the real setup is beyond the scope of this article. It is worth noting that numerical modeling of such phenomena without our model is an irksome job since (i) time-domain Maxwell equation solvers require a prohibitive computational effort and (ii) coupled wave approaches cannot be used in the presence of overlapping frequency bands of different field components.

IV. CONCLUSIONS

In conclusion we have derived a robust nonlinear envelope equation describing the propagation in dispersive quadratic materials. Owing to a proper formal definition of the complex envelope, it is possible to treat pulses of arbitrary frequency content. A proper definition of the envelope is crucial for second-order nonlinearities, due to the generation of frequency components around zero. Previous works [2–7], which were more focused on cubic nonlinearities, did not consider this aspect. Computationally it is possible to accurately evolve optical pulses of arbitrarily wide band over a meter-scale physical distance, which is a few orders of magnitude longer than those accessible by Maxwell equation solvers.

[1] R. W. Boyd, *Nonlinear Optics*, 2nd ed. (Academic, New York, 2003).
[2] T. Brabec and F. Krausz, Phys. Rev. Lett. **78**, 3282 (1997).
[3] T. Brabec and F. Krausz, Rev. Mod. Phys. **72**, 545 (2000).
[4] M. Geissler *et al.*, Phys. Rev. Lett. **83**, 2930 (1999).
[5] A. V. Husakou and J. Herrmann, Phys. Rev. Lett. **87**, 203901 (2001).
[6] M. Kolesik, J. V. Moloney, and M. Mlejnek, Phys. Rev. Lett. **89**, 283902 (2002).
[7] G. Genty, P. Kinsler, B. Kibler, and J. M. Dudley, Opt. Express **15**, 5382 (2007).
[8] A. A. Kanashov and A. M. Rubenchik, Physica D (Amsterdam) **4**, 122 (1981).
[9] P. Kinsler and G. H. C. New, Phys. Rev. A **67**, 023813 (2003).
[10] J. Moses and F. W. Wise, Phys. Rev. Lett. **97**, 073903 (2006).
[11] C. Langrock, M. M. Fejer, I. Hartl, and M. E. Fermann, Opt. Lett. **32**, 2478 (2007).
[12] S. Haykin, *Communication System*, 4th ed. (Wiley, New York, 2001).
[13] A. Bruner *et al.*, Opt. Lett. **28**, 194 (2003).
[14] M. Conforti, F. Baronio, and C. De Angelis, Opt. Lett. **32**, 1779 (2007).
[15] D. H. Jundt, Opt. Lett. **22**, 1553 (1997).